Ion Conduction through C-Type Inactivated *Shaker* Channels

John G. Starkus,*‡ Lioba Kuschel,* Martin D. Rayner,§ and Stefan H. Heinemann*

From the *Research Unit Molecular and Cellular Biophysics, Max Planck Society, D-07747 Jena, Germany; ‡Békésy Laboratory of Neurobiology, Pacific Biomedical Research Center, and §Department of Physiology, School of Medicine, University of Hawaii, Honolulu, Hawaii 96822-2359

ABSTRACT C-type inactivation of *Shaker* potassium channels involves entry into a state (or states) in which the inactivated channels appear nonconducting in physiological solutions. However, when *Shaker* channels, from which fast N-type inactivation has been removed by NH_2-terminal deletions, are expressed in *Xenopus* oocytes and evaluated in inside-out patches, complete removal of K^+ ions from the internal solution exposes conduction of Na^+ and Li^+ in C-type inactivated conformational states. The present paper uses this observation to investigate the properties of ion conduction through C-type inactivated channel states, and demonstrates that both activation and deactivation can occur in C-type states, although with slower than normal kinetics. Channels in the C-type states appear "inactivated" (i.e., nonconducting) in physiological solutions due to the summation of two separate effects: first, internal K^+ ions prevent Na^+ ions from permeating through the channel; second, C-type inactivation greatly reduces the permeability of K^+ relative to the permeability of Na^+, thus altering the ion selectivity of the channel.

KEY WORDS: potassium channels • channel inactivation • ion selectivity • patch clamp • *Xenopus* oocyte

INTRODUCTION

Inactivation in both sodium and A-type potassium channels (K^+ channels) can be separated into two forms with different putative mechanisms. Thus, in sodium channels, fast inactivation is sensitive to pronase (Armstrong et al., 1973), although slow inactivation is not (Rudy, 1978). Further, the simple kinetics and low independent voltage sensitivity of fast inactivation in Na^+ channels lead Armstrong and Bezanilla (1977) to suggest their "ball and chain" hypothesis. This hypothesis has since been confirmed as the mechanism of fast (N-type) inactivation in *Shaker* K^+ channels at the structural level (Hoshi et al., 1990; Zagotta et al., 1990). However, the mechanisms underlying the slower, pronase-resistant inactivation processes (Hoshi et al., 1991) are less well understood, although recent evidence has clarified that structural changes occur in the outer mouth of the *Shaker* channel during this slow (C-type) inactivation (Liu et al., 1996; Schlief et al., 1996). These changes were interpreted as indicating a collapse of the external channel mouth, which occludes the ion permeation pathway.

On the other hand, previous studies have reported conduction of normally impermeant monovalent cations (e.g., Na^+ and Li^+) through delayed rectifier K^+ channels (Callahan and Korn, 1994; Ikeda and Korn, 1995) after removal of K^+ ions from both internal and external solutions. Similarly, Na^+ permeation has been reported through noninactivated *Shaker* channels (Ogielska and Aldrich, 1997) after K^+ ions have been removed from the internal solution. The present study extends these observations to include permeation of Na^+ and Li^+ ions through C-type inactivated *Shaker* channels. Thus, we demonstrate that even channels that have become impermeant to K^+ ions are capable of conducting normally impermeant monovalent cations after the careful removal of internal K^+. If C-type inactivated channels can conduct these ions in K^+-free internal solutions, then the mechanism of C-type inactivation is unlikely to involve a structural collapse affecting the conduction pathway. Moreover, the finding that permeation of Na^+ or Li^+ can be blocked by submillimolar concentrations of internal K^+ ions suggests the presence of a high affinity K^+ binding site at the internal surface of the permeation path, where K^+ binding contributes to the blockade of "impermeant" ion species.

We propose here that conduction through *Shaker* channels is determined by summation of two different regulatory effects: first, there is the internal K^+ ion effect that appears similar in both normal and C-type inactivated channels. This effect prevents significant permeation by Na^+ or Li^+ ions when K^+ ions are present in the internal solution. Second, there is an external site that changes its conformation on entry into C-type inactivated states. This outer site is normally highly selective for K^+ over Na^+, but, during C-type inactivation,

Preliminary results of this work have been presented in abstract form (Heinemann, S.H., J.G. Starkus, and M.D. Rayner. 1997. *Biophys. J.* 72:*A*29; Starkus, J.G., M.D. Rayner, and S.H. Heinemann. 1997. *Biophys. J.* 72:*A*232).

Address correspondence to Stefan H. Heinemann, Research Unit Molecular and Cellular Biophysics, Max Planck Society, Drackendorfer Str. 1, D-07747 Jena, Germany. Fax: 49 3641 304 542; E-mail: ite@rz.uni-jena.de

the structurally modified outer site prevents permeation of K^+ but not of Na^+ ions. Thus, in normal physiological solutions, C-type inactivation results in *Shaker* channels becoming functionally impermeable to all available ion species, since the outer site becomes impermeable to K^+ ions while internal K^+ ions prevent Na^+ permeation.

MATERIALS AND METHODS

Channel Expression

All studies reported here were carried out using the *Shaker* D 29-4 construct (Iverson and Rudy, 1990) in which fast, N-type inactivation has been removed by deletion of the residues 2–29 (McCormack et al., 1994; this construct will be referred to as *Sh*Δ). Oocytes of *Xenopus laevis* were surgically obtained under tricaine/ice water anesthesia. Follicular layers were removed according to standard methods. mRNA was synthesized in vitro and was injected into *Xenopus* oocytes at a concentration ranging from 0.005 to 0.1 μg/μl (total volume ~50 nl per oocyte). Oocytes were incubated at 18°C for 1–7 d before electrophysiological recordings.

Electrophysiology

All data reported here were obtained in inside-out macropatch recordings (Hamill et al., 1981) using either an EPC-7 or EPC-9 patch clamp amplifier (HEKA Elektronik, Lambrecht, Germany). Patch pipettes were fabricated from aluminum silicate or borosilicate glass, yielding resistances in standard solutions between 0.5 and 2 MΩ. Data acquisition was controlled with the Pulse+PulseFit software package (HEKA Elektronik). Experiments were carried out at room temperature ranging between 20 and 22°C. Data analysis was performed with PulseFit, PulseTools (HEKA Elektronik) and IgorPro (Wave Metrics, Lake Oswego, OR) software. Leak and capacitive transients were compensated using a variable P/*n* correction (Heinemann et al., 1992) with a typical leak holding potential of −120 mV. In several cases, leak and capacitive transients were eliminated by off-line leak correction methods. Unless otherwise stated, data values are specified as mean ± SD (n = number of independent experiments).

Where appropriate, estimates of the effective voltage sensitivity of transitions in the deactivation or reactivation pathways were obtained by fitting time constant–voltage curves to the following relationship: $\tau(V) = \tau(0) \exp(\pm Vq/kT)$, where $\tau(V)$ is the observed time constant at the applied transmembrane voltage, V; k is Boltzmann's constant, T is the absolute temperature, and q is the apparent charge moved between the appropriate thermodynamic energy well and the energy barrier for the transition in question.

As all experiments were done in the inside-out configuration, only the intracellular bath solution could be changed in individual patches. Solution changes were carried out either (*a*) by exchange of the entire bath volume (taking ~1 min), or (*b*) via a valve-operated quartz-capillary manifold where the pipette tip was positioned in the manifold outlet. This second method permitted solution changes within ~100 ms. Great care had to be taken in carrying out solution exchanges in order to ensure effective removal of residual K^+ from earlier bath solutions, from close proximity of the patch to the oocyte surface, or from cytoplasm adhering to a freshly excised inside-out patch.

Solutions

In addition to monovalent chloride salt, external solutions always contained 1.8 mM $CaCl_2$ and 10 mM HEPES, pH 7.2. Internal solutions contained 1.8 mM EGTA and 10 mM HEPES, pH 7.2. The solutions were named according to the content of monovalent cations. External (mM): Normal Frog Ringer (NFR),[1] containing 115 NaCl and 2.5 KCl; K-Ringer, containing 115 KCl; Na-Ringer, containing 115 NaCl; Li-Ringer, containing 115 LiCl; Tris-Ringer, containing 115 TrisCl. Internal (mM): K-EGTA, containing 115 KCl; Na-EGTA, containing 115 NaCl; Tris-EGTA, containing 115 TrisCl.

Combinations of these monovalent cations were obtained by appropriate mixing of these solutions. In the text and figures, the solutions are only specified by the concentrations of the monovalent cations: external/internal solution.

RESULTS

Deletion of the residues that constitute the NH_2-terminal "ball" domain has made it possible to generate *Shaker* channel constructs with otherwise normal properties, but in which fast, N-type inactivation has been completely eliminated (Hoshi et al., 1990). However, although the onset of C-type inactivation is extremely slow in high K^+ extracellular media, this onset rate is accelerated by reducing extracellular K^+ concentration or by substitution with other extracellular monovalent cations following the order $K^+ < Rb^+ << Na^+$, Cs^+, NH_4^+ (López-Barneo et al., 1993; Levy and Deutsch, 1996). Onset of inactivation is further accelerated when internal as well as external K^+ concentration is reduced by impermeant ion substitutions. Thus, even channels in which N-type inactivation has been removed by deletion of the NH_2-terminal ball domain can inactivate in K^+-free media with a time course in the tens of milliseconds range in symmetric Na^+ solutions (see Fig. 1 *F*). This rate is approximately equivalent to the rate of normal fast N-type inactivation in physiological solutions and is almost three orders of magnitude faster than the rates of C-type inactivation in high external K^+ media. Clearly, a question that must be addressed here is whether this very fast inactivation process shares a common mechanism with the slow C-type inactivation previously characterized in more physiological solutions.

Fig. 1, *A–C* presents the previously characterized effects of extracellular K^+ in modulation of the onset rate of C-type inactivation. Fig. 1 *A* demonstrates the slow onset of inactivation in symmetric K^+ solutions as compared with the faster onset in more physiological media (Fig. 1 *B*). Onset rate is further increased when K^+ is removed from the external medium by $Tris^+$ substitution (Fig. 1*C*). The trace shown in Fig. 1*C* further suggests that steady state is approached after ~3 s at +40 mV.

[1]*Abbreviations used in this paper:* I-V, current–voltage; NFR, Normal Frog Ringer.

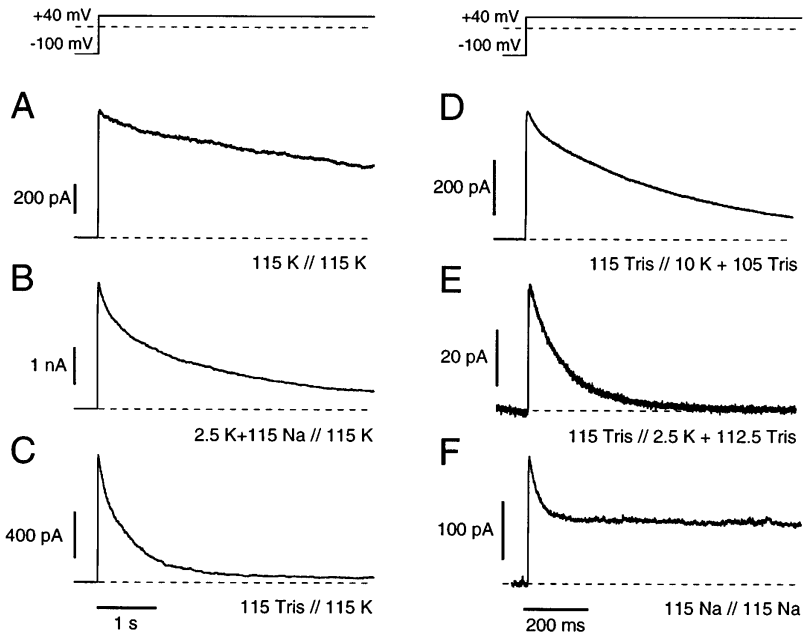

FIGURE 1. C-type inactivation rate is affected by changes in external (*A–C*) and internal (*D–F*) cation concentrations, as shown using inside-out macro-patch recordings from *Sh*Δ channels. The potential profile is indicated at the top and the current traces were digitally low pass filtered at 1 kHz. (*A*) K-Ringer versus K-EGTA. (*B*) NFR versus K-EGTA. (*C*) Tris-Ringer versus K-EGTA. (*D*) Tris-Ringer versus 10 mM KCl, 105 mM TrisCl, 1.8 mM EGTA. (*E*) Tris-Ringer versus 2.5 mM KCl, 112.5 mM TrisCl, 1.8 mM EGTA. (*F*) Na-Ringer versus Na-EGTA. Single-exponential fits (see text) resulted in the following time constants: 9.3 s, 1.6 s, 550 ms, 520 ms, 120 ms, and 31 ms in *A–F*, respectively. In *F*, the current reached a steady state level that was 50% of the peak current.

Although the time course of C-type inactivation is voltage independent in physiological solutions, this inactivation rate cannot be fully characterized by single exponentials (López-Barneo et al., 1993; Meyer and Heinemann, 1997). An initial, faster component of inactivation is particularly noticeable in Fig. 1, *A–C*. Nevertheless, after the decay of this initial component, single time constants well fit the remaining inactivation time course and indicate the sensitivity of this slow inactivation mechanism to extracellular K^+ ions (for time constants, see figure legend).

Fig. 1, *D–F* shows the effects of reducing internal K^+ concentration on the onset rate of C-type inactivation (note the expanded time base for these records). With external cations substituted by $Tris^+$ and internal K^+ concentration reduced from 115 to 10 mM (Fig. 1 *D*) and to 2.5 mM (Fig. 1 *E*), the inactivation time constant further decreases. Complete substitution of internal K^+ ions using symmetric 115 mM internal and external Na^+ solutions (Fig. 1 *F*) again decreases the inactivation time constant to ~30 ms, and outward I_{Na} inactivates to a steady state level of ~50% of peak I_{Na} at +40 mV. This steady state Na^+ current is larger relative to peak I_{Na} at less positive test potentials, although the observed current increases monotonically with increasing test potential (data not shown).

Since these records were obtained using leak subtraction, the outward steady state I_{Na} must be occurring either through residual noninactivated channels or through inactivated channels or some mix of normal and inactivated channels. Although this result shows that Na^+ can pass through *Sh*Δ channels (after removal of internal K^+), it is not yet clear that inactivated channels are involved in generation of these steady state Na^+ currents. We have addressed this important question through several different approaches.

Effects of Test Pulse Duration on Na^+ Tail Currents

Fig. 2 compares the development of C-type inactivation during the test pulse with the changing time course of inward Na^+ tail currents using records obtained in K^+-free solutions. In Fig. 2 *A*, using symmetric 115 mM Na^+ solutions where the test pulse potential was +40 mV for direct comparability with Fig. 1 *F*, tail currents show fast kinetics at the shortest test pulse duration (2 ms) when the repolarizing step is initiated on the rising phase of the outward Na^+ current. However, with increasing test pulse duration, and consequently increasing C-type inactivation, this initial fast tail current component is progressively reduced as a slower component develops in the tail current decay. Thus, after a 64-ms test pulse (the longest duration shown here), the fast component entirely disappears and a pronounced rising phase (or "hook") becomes apparent in this tail current.

In Fig. 2 *B*, the internal Na^+ concentration was adjusted to 38 mM (plus 77 mM Tris) such that the test potential (here +20 mV) would be close to the Na^+ reversal potential. Thus, the outward current is primarily gating current (Ig_{ON}), permitting clear determination that ionic conductance is the major contribution to these tail currents (i.e., the ratio of the OFF/ON integrals is significantly greater than unity). As in Fig. 2 *A*, at the shortest test pulse duration there is a fast initial decay followed by a long slow relaxation component.

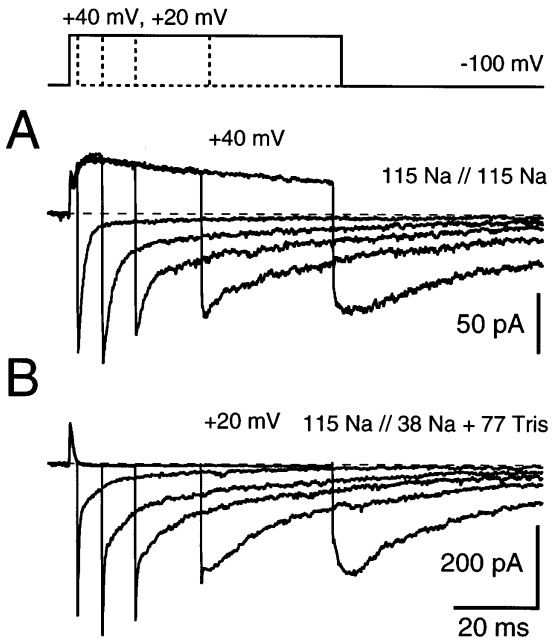

FIGURE 2. Tail current kinetics change as C-type inactivation develops (*A* and *B*). *(A)* Recordings obtained in symmetric (115 mM) Na^+ solutions, using test pulses (to +40 mV) of differing durations demonstrate that development of C-type inactivation parallels significant changes in tail current waveform. After short depolarizations, they are dominated by a rapid component associated with deactivation of noninactivated channels, followed by a small slow ionic component. This slow ionic current component increases with increasing depolarization duration. Finally, a rising phase (hook) in the onset of the slow ionic current becomes apparent while the initial, fast peak disappears as C-type inactivation approaches steady state. *(B)* Recordings obtained under ionic conditions where the estimated reversal potential for Na^+ (115 mM versus 38 mM) nearly matches the potential of depolarization (+20 mV) such that Ig_{ON} becomes clearly visible. Upon increasing duration of the depolarizing pulse segment, the tail currents undergo kinetic changes similar to those seen in *A*. Data traces were low pass filtered at 4 kHz.

As the pulse duration increases, the initial fast decay decreases in magnitude while there is a corresponding increase in the slow component. Disappearance of the fast component at the longest test-pulse duration shown here (64 ms) again reveals a substantial slow rising phase in the Na^+ tail current. Noting that the loss of the fast component corresponds to the time course of C-type inactivation (Figs. 1 *F* and 2 *A*), the slow tail current component appears likely to represent deactivation of a Na^+ current that is occurring through C-type inactivated channels.

However, it is also possible that noninactivated channels may change their deactivation rate for reasons unrelated to the coincident inactivation process, or that inactivated channels become conducting during recovery from C-type inactivation. Finally, we have already raised the concern that this very fast, non–N-type inactivation might be different in its mechanism from the dominant C-type inactivation seen in more physiological solutions, despite the lack of any pronounced discontinuity in the rates seen in Fig. 1 between the slow inactivation rate in symmetric K^+ solutions (Fig. 1 *A*) and records with reduced K^+ concentration (Fig. 1, *B–F*).

Effects of Test Pulse Duration on Tail Currents in the Presence of External K^+

To address the questions raised above, we repeated a pulse-duration study using external solutions containing either 2.5 mM K^+ plus 115 mM $Tris^+$ (Fig. 3, *A* and *B*) or 2.5 mM K^+ plus 115 mM Na^+ (Fig. 3, *C* and *D*). In both cases, the internal solution was Tris-EGTA (see MATERIALS AND METHODS). Fig. 3, *A* and *C* shows superimposed current traces yielding various degrees of inactivation at the end of the depolarization. Fig. 3, *B* and *D* shows the tail currents on an expanded time base and aligned in time to the end of the depolarizing pulse. In Fig. 3 *A*, with no external Na^+, it is clear that the tail currents are fast at all prepulse durations and are markedly reduced coincident with the onset of C-type inactivation (visible from the decay of the inward K^+ current at −20 mV). These tail currents are reduced to little more than the expected magnitude of Ig_{OFF} by the time C-type inactivation reaches a steady state. Clearly, channels do not conduct K^+ ions to any significant extent in the C-type inactivated state. By contrast, if 115 mM Na^+ is added to the external solution, as in Fig. 3 *C*, two effects are seen. First, fast tail currents are visible at shorter prepulse durations, but are gradually replaced during the course of C-type inactivation by slow tail currents that no longer diminish in size. In Fig. 3 *D* we see that these tail currents develop the characteristic rising phase with a time course similar to that of C-type inactivation. This relationship between the development of C-type inactivation and the increase in the slow tail current peak is shown to be linear in Fig. 3 *E*. Second, Fig. 3 *C* shows a substantial increase in the inward steady state current in the presence of external Na^+ ions.

One hypothesis would be that the entire slow tail currents of Fig. 3, *B* and *C* are being generated by K^+ permeation through channels that recover rapidly from C-type inactivation at negative potentials in the presence of external Na^+ ions, but which do not recover in the absence of external Na^+ (Fig. 3 *A*). This hypothesis predicts that the slow tail currents should return to baseline only when channels fully recover from C-type inactivation. Thus, recovery should be complete within 0.5 s at −100 mV return potential. By contrast, we find that recovery from C-type inactivation is still incomplete after a 3-s return to −100 mV, even in 115 mM external Na^+ solution (data not shown).

It might seem reasonable, therefore, to presume that these tail currents represent Na^+ permeating through C-type inactivated channels, in the absence of blocking effects that would normally be generated by intracellu-

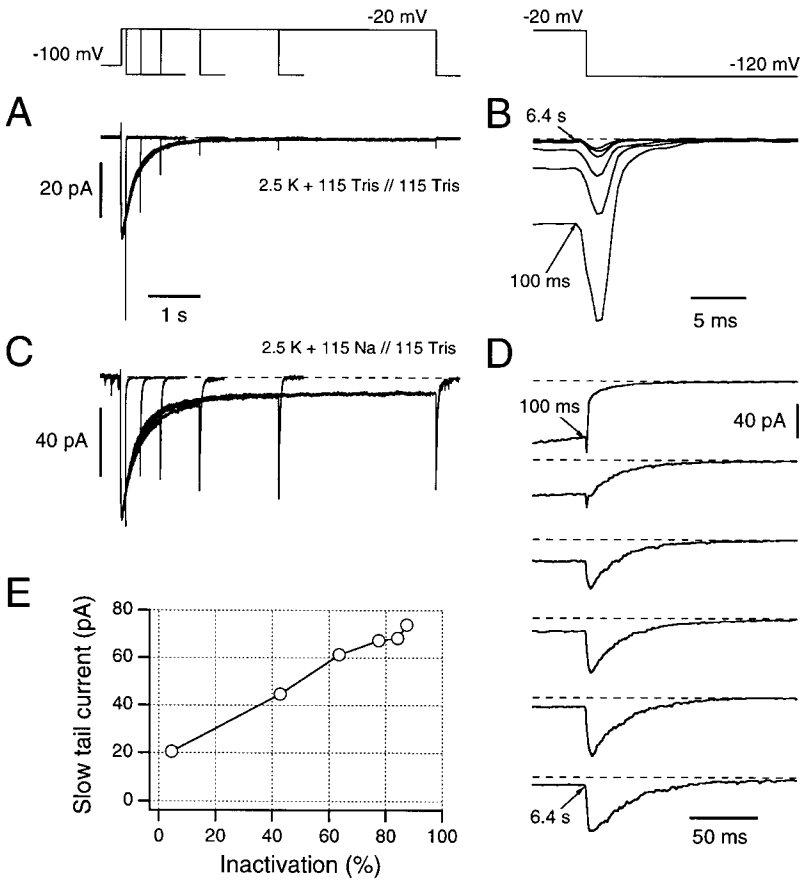

FIGURE 3. Dependence of inward tail current waveforms on the development of C-type inactivation, without (*A* and *B*) and with (*C* and *D*) addition of external Na^+ ions. Inward currents were measured in the absence of intracellular permeating ions (Tris-EGTA in the bath), during pulses to −20 mV in external 2.5 mM K^+ plus 115 mM Tris (*A* and *B*) or in NFR containing 2.5 mM K^+ plus 115 mM Na^+ (*C* and *D*). In these solutions, channels inactivate with a time constant of ~1 s. In the absence of Na^+ (*A*), the tail currents upon repolarization to −120 mV are rapid and decrease in magnitude as the degree of inactivation increases (see *B*). In the presence of external Na^+ (*C*), however, tail currents are only rapid after very brief depolarizations. After longer depolarizations (i.e., as C-type inactivation occurs), tail currents slow down and do not decrease in size. *D* shows the tail current sections of *C*, aligned in time to the end of the test depolarization. Note the 10-fold change in time scale compared with *B*. *E* shows an analysis of data from *C* and *D*, demonstrating a linear relationship between the fraction of channels that have entered into C-type inactivation and the peak magnitude of the slow component of Na^+ tail currents.

lar K^+ ions (Callahan and Korn, 1994; Ikeda and Korn, 1995). In the next section, we address the question as to whether or not any change in the permeating ion species occurs coincident with the onset of C-type inactivation.

Ion Permeation through C-Type Inactivated Channels in K^+-free Internal Solutions

The central hypothesis to be evaluated in this section is that *Shaker* channels change their relative permeabilities for K^+ and Na^+ as they enter into the C-type inactivated state(s). Thus, we question whether they progress from their normal K^+-selective state into a C-type state in which they are no longer permeant to K^+ ions, although they remain permeable to Na^+ ions (as long as the blocking action of intracellular K^+ can be prevented, see below). If this hypothesis is correct, and if channels are provided with an external solution that contains both K^+ and Na^+ ions, then noninactivated channels would be primarily K^+ conductors, whereas inactivated channels should be either nonconducting or Na^+ conducting, depending on the presence or absence, respectively, of K^+ in the internal solution. This prediction could be tested if it were possible to report which ion species were the primary current carriers at different times during a long, inactivating test pulse.

We have explored this possibility by evaluating the instantaneous current–voltage relationship in carefully chosen internal and external solutions. With an external solution containing 2.5 mM K^+ and 115 mM Na^+ and a K^+-free internal solution (also containing 115 mM Na^+), the reversal potential for K^+-conducting channels should be >+50 mV, whereas the reversal potential for Na^+-conducting channels should be close to 0 mV. Thus, after a test pulse to −20 mV, either steps to appropriate return potentials or voltage ramps can be used to evaluate the reversal potential seen at different test pulse durations. In either case, it should be possible to demonstrate whether or not the hypothesized change in relative permeabilities occurs, as C-type inactivation develops during the test pulse. The predicted result will be a progressive left shifting of the reversal potential, from ~+50 mV towards less positive potentials, coincident with development of C-type inactivation.

The standard instantaneous current–voltage (I-V) procedure is demonstrated in Fig. 4 *A*, in which "tail" steps to both +40 and −40 mV were applied after the patches were depolarized to −20 mV for either 200 ms or 3 s. After the short (200-ms) test pulse in which ~10% of peak inward current has become C-type inactivated, the step to −40 mV generates a composite tail current with both fast and slow components, whereas the step to

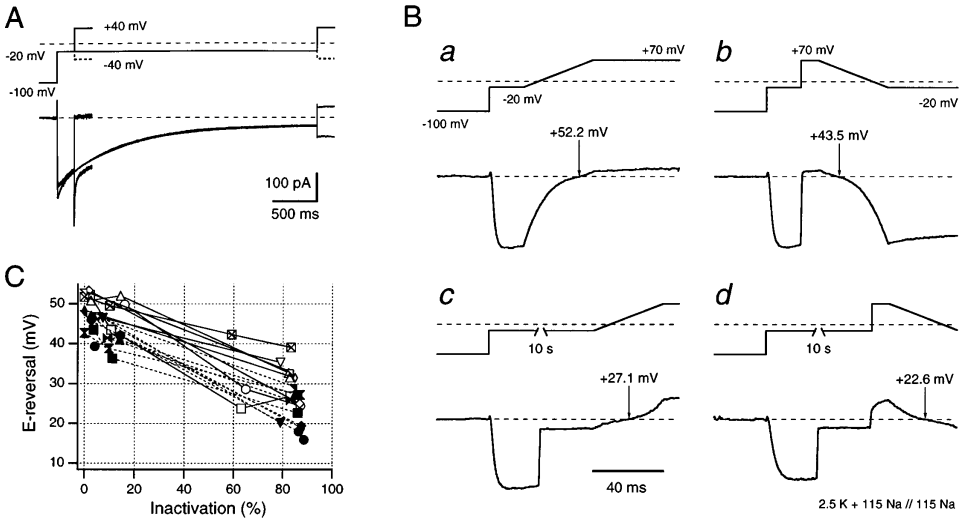

FIGURE 4. *Shaker* channels become less permeable to K^+ ions and relatively more permeable to Na^+ ions when C-type inactivated. (*A*) Superposition of four current traces recorded in NFR versus Na-EGTA; i.e., in symmetrical 115 mM Na^+ but with 2.5 mM K^+ added to the external solution. Pairs of traces were recorded with a depolarization to −20 mV for 200 ms and 3 s leading to quite different degrees of inactivation at the end of the depolarization. Subsequently, the potential was stepped to either −40 or +40 mV. After the short depolarization, the subsequent step to +40 mV shows only marginal outward current, the same step after almost complete inactivation results in outward currents that are ~50% of the size of the inward currents obtained at −40 mV, indicating an enhanced relative Na^+ permeation after development of C-type inactivation. (*B*) Demonstration of the protocol used for collection of instantaneous I-V data at two different durations within a −20-mV test depolarization. Ramp potential changes of 40-ms duration were imposed after 20-ms (*B, a* and *b*) and 10.04-s (*B, c* and *d*) test pulses. Ramps were upward (from −20 to +70 mV) in *B, a* and *c*, and downward (from +70 to −20 mV) in *B, b* and *d*. See text for further description of this protocol. (*C*) Reversal potentials obtained from instantaneous I-V data are plotted as functions of the degree of C-type inactivation that had occurred before starting the ramps. Results are shown for eight patches from which full data sets were collected. Straight lines connect data points from the same patch. Upward ramp data points are shown by open symbols and connected by solid lines, downward ramp points are shown by filled symbols and connected by dashed lines.

+40 mV reaches the zero current baseline, as if the effective reversal potential is ~+40 mV at this early stage in the onset of C-type inactivation. However, after the long (3-s) test pulse, in which some 90% of peak current has been eliminated by C-type inactivation, the tail current in the +40-mV step is now clearly outwardly directed, whereas the tail current is still inward at −40 mV. As a first approach, linear interpolation between these outward and inward tail currents suggests a reversal potential of ~+15 mV at this time. Comparing these tail currents imposed at different points in the development of C-type inactivation suggests that the reversal potential changes in the direction predicted by our hypothesis.

Unfortunately, problems occur in using the simple approach described above for careful, quantitative studies. Long interpulse intervals are required to prevent accumulation of C-type inactivation and it is not easy to complete the number of pulses required to obtain accurate measures of reversal potentials at both short and long times in the same patch. This method was, therefore, modified by inserting voltage ramps (between −20 and +70 mV) in which the instantaneous I-V data could be directly visualized within the 40-ms time course of each ramp. Additionally, both increasing (−20 to +70 mV) and decreasing (+70 to −20 mV) ramps were used to evaluate any possible directional artifacts in this method. These voltage-ramp protocols are illustrated in Fig. 4 *B*, which shows four instantaneous I-V plots that were obtained from a single patch.

Fig. 4 *B*, *a* and *b* indicates the results obtained in the solutions described above, after a 20-ms prepulse to −20 mV and (Fig. 4 *B*, *c* and *d*) after a 10.04-s prepulse. Note that traces *c* and *d* do not show the complete time course of the current record, a 10-s interval was inserted in the pulse paradigm, where indicated, in which data traces were not digitized, yielding a more faithful P/*n* leak correction (Steffan et al., 1997). Upward ramps from −20 to +70 mV are shown in Fig. 4 *B*, *a* and *c*, while downward ramps from +70 to −20 mV are shown in traces *b* and *d* (after a depolarizing step from the −20-mV test potential to +70 mV, and a brief preramp delay of 10 ms). Voltage protocols are shown above the current records in each panel. Thus, for each test pulse duration, the observed reversal potential could be evaluated from the leak-subtracted currents seen during both upwardly and downwardly directed voltage ramps. In the patch shown here, after the 20-ms prepulse, reversal potential was +52.2 or +43.5 mV depending on ramp direction (Fig. 4 *B*, *a* and *b*), whereas after 10.04 s, the corresponding values were +27.1 and +22.6 mV (Fig. 4 *B*, *c* and *d*). Fig. 4 *C* shows the cumulative data obtained from eight different patches using ramps in both directions, plotted against the degree of C-type inactivation obtained by the depolarization to −20 mV before the start of each ramp protocol. In this figure, the mean reversal potential shifts to the left by ~26 mV with increasing C-type inactivation, as predicted by the hypothesis stated above.

Quantitative errors in this data set could arise from

two principal sources. First, in view of the low external K^+ concentration (2.5 mM), any significant accumulation of internal K^+ ions during the long prepulse to −20 mV might be expected to lower the reversal potential at long times. However, such K^+ accumulation would also block Na^+ permeation (see below), thus obscuring the major shift of reversal potential predicted by the data shown in Fig. 4. To address this problem, inside-out patches were positioned in the direct path of a pipette perfusing the Na-EGTA internal solution so as to minimize any possible accumulation of internal K^+. In addition, any effect due to K^+ accumulation should be much smaller in protocols using downward ramps. Second, changes in the extent of steady state C-type inactivation could occur during voltage ramps between −20 and +70 mV, altering the fraction of noninactivated channels remaining after long prepulse duration. This problem was minimized by using short (40 ms) ramps with only a short delay of 10 ms at +70 mV before the start of the down ramp. The estimated reversal potentials in the absence of inactivation at the start of the ramp protocol were 51.4 ± 1.5 mV for upward ramps and 44.8 ± 1.1 mV for downward ramps, indicating that this difference is indeed caused by additional inactivation induced by the preramp delay of 10 ms at +70 ms used for the downward ramps. Nevertheless, the measured shifts of the reversal potential as a function of inactivation are highly significant for both protocols. The inactivation-induced reduction in reversal potential between partially and completely inactivated channels was 26.2 ± 2.0 mV for downward ramps (Fig. 4 *C*, *closed symbols*) and 25.8 ± 2.5 mV for upward ramps (Fig. 4 *C*, *open symbols*), providing strong confirmation for the hypothesis presented above.

Finally, it may seem surprising, initially, that the reversal potential at long times does not move closer to 0 mV than ~+25 mV. However, the relative permeability of Na^+ versus K^+ (P_{Na}/P_K) is normally ~0.02 in *Shaker* channels; moreover, P_{Na} falls rather than increases during C-type inactivation (see Fig. 1 *F*). Thus, even if 98% of the channels become inactivated, Na^+ flux through those channels would be expected to be not greater than the K^+ flux occurring through the remaining 2% of noninactivated channels. Hence, the reversal potential data suggest that, at long test pulse durations, an equilibrium becomes established between normal and C-type inactivated channels such that some very small fraction of residual noninactivated channels remains, even after 10 s at −20 mV.

Conduction through C-Type Inactivated Channels Is Blocked by Internal K^+

We next demonstrate the blocking of ion conduction through C-type inactivated channels by internal K^+ ions. Fig. 5 explores the effects of washout of K^+ ions from the internal medium. Fig. 5, *i* was obtained using Li-Ringer (see MATERIALS AND METHODS) as the external solution and with 5 mM of K^+ in the $Tris^+$-substituted internal solution. Test pulse duration was 40 ms, which is long enough to produce considerable C-type inactivation in K^+-free solutions (see Fig. 1 *F*). However, with 5 mM of K^+ in the internal solution, it is clear that little C-type inactivation takes place during this short pulse and Ig_{OFF} is clearly seen here as part of the tail currents (see arrow). The remaining traces (Fig. 5, *ii–iv*) show successive records obtained during slow washout of the internal solution with K^+-free Tris-EGTA solution. As the internal K^+ concentration falls, the peak outward current also falls and the fraction of channels that become C-type inactivated within the 40-ms duration of the test pulse increases (as assessed from $[I_{peak} - I_{40\ ms}]/I_{peak}$). When the outward K^+ current has been reduced by approximately one order of magnitude (see Fig. 5, *iii*) compared with the original record in 5 mM K^+, the Li^+ tail current starts to show the slow rising phase as seen in Fig. 2, which is characteristic of tail currents through C-type inactivated channels. A further increase in the slow tail peak occurs in trace *iv*, associated with additional loss of outward K^+

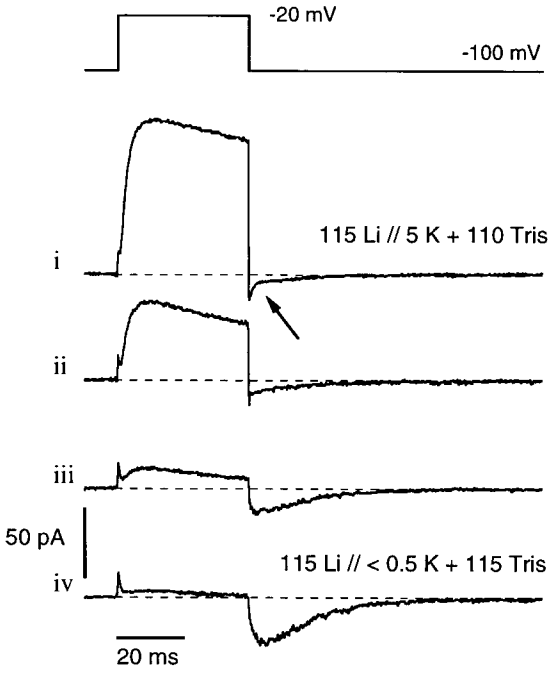

FIGURE 5. Influence of intracellular K^+ on the tail currents. The first trace (*i*) was recorded with external Li-Ringer (same results would be obtained with Na^+ instead of Li^+ as permeating ion, not shown) and an internal solution containing 5 mM K^+ plus 110 mM $Tris^+$. The arrow points to an inflection in the tail currents indicating two components. The following traces (*ii–iv*) were recorded while the internal K^+ ions were slowly washed out by Tris-EGTA solution. As the outward currents disappear, due to removal of internal K^+ ions, the tail currents become slower and larger, indicating increased Li^+ permeation.

current and presumably a further reduction in internal K^+ concentration.

Activation and Deactivation in C-Type Inactivated Channels

We have seen that *Sh*Δ channels can show steady state conductance after entering into C-type inactivated states (Figs. 1 *F*, 3 *C*, and 4) and that they can generate slow tail currents while apparently deactivating in C-type inactivated states (Figs. 2 and 3 *D*). At these negative return potentials, Na^+ current decays to zero. Since the duration of the hooked tail currents (<500 ms) is at least one order of magnitude less than the time required for full recovery from C-type inactivation (>5 s), we presume that these channels are deactivating to a closed C-type state. On the other hand, the "closed C-type state" reached in this apparent deactivation may not be the same as the normal closed state, and the hook in these tail currents implies an additional process occurring before the channel closing step. Furthermore, the fast tail currents of noninactivated channels fail to provide any kinetic evidence to indicate a corresponding "preclosing" transition. Is the deactivation of C-type inactivated channels in any way comparable with the deactivation of noninactivated channels?

This question is addressed in Fig. 6. In Figs. 6 *A* and, particularly, *B*, where the same experiments are presented on a faster time base, it is apparent that the rising phase (or hook) follows an initial increase in inward current resulting from a change of driving force before the settling of the voltage clamp. After the clamp has settled (in <200 μs), we see a slower increase in tail current amplitude that we presume reflects either some process specific to the C-type inactivated state, relief of divalent ion block, or, alternatively, a rapid initial component of recovery from C-type inactivation. Further work will be required to distinguish between these possibilities.

The rising and falling phases of these tail currents were analyzed by fitting double exponential functions to leak-subtracted data. In Fig. 6 *C*, the rising and falling phase time constants, τ_{Cd1} and τ_{Cd2}, respectively, are plotted on a logarithmic scale against return potential. At the most negative return potentials, the voltage sensitivities of the two time constants in Na/Na solutions correspond to an apparent charge movement of 0.51 ± 0.05 and 1.05 ± 0.03 e_0 for τ_{Cd1} and τ_{Cd2}, respectively (see MATERIALS AND METHODS). The estimated time constants at 0 mV were 6.1 ± 1.5 s and 884 ± 134 ms for τ_{Cd1} and τ_{Cd2}, respectively ($n = 6$). Under asymmetrical conditions (Na/Tris), the voltage sensitivities were 0.53 ± 0.08 and 1.13 ± 0.11 e_0, and the estimated time constants at 0 mV were 13.5 ± 6.2 s and 5.2 ± 2.7 s ($n = 5$). Interestingly, the slopes for τ_{Cd2} are similar to reported values for normal tail currents (Zagotta et al., 1994*a*), although the time constants are considerably slower than is normal for *Shaker* tail currents at similar potentials. These results suggest that both rising (τ_{Cd1}) and falling (τ_{Cd2}) transitions are driven by voltage-sensitive processes.

Recovery from C-type inactivation is not complete for at least 5 s at −100 mV in K^+-free solutions, although tail current deactivation closes all channels within 500 ms. Therefore, it seems reasonable that these channels might reactivate, although to the reduced permeability characteristic of depolarized C-type states, when a second test depolarization is applied before significant recovery from C-type inactivation has occurred. As demonstrated in Fig. 7 *A*, recovery from C-type inactivation is affected by the ionic content of the external solution

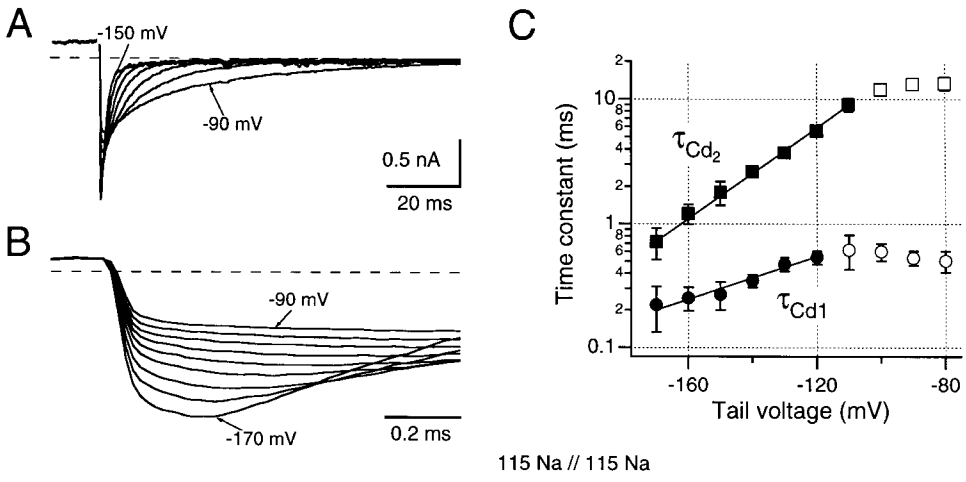

FIGURE 6. Deactivation of C-type inactivated channels. (*A* and *B*) Tail currents were recorded after depolarizations to +20 mV for 100 ms at tail potentials between −170 and −80 mV using 10-mV steps. Representative traces are shown in *A* and *B* using different time scales to demonstrate the voltage sensitivity of deactivation in *A* and of the hooked rising phase in *B*. The recording bandwidth was 4 kHz. The time constants of both, the hooks (τ_{Cd1}) and the deactivation (τ_{Cd2}), were estimated by fitting double-exponential functions to the data. The mean time constants resulting from six experiments are plotted in *C* as a function of the tail potential. The filled symbols indicate those data points that were considered for the determination of the slopes (*straight lines*) that yielded a voltage dependence for both processes corresponding to effective gating valences of 0.51 (τ_{Cd1}) and 1.05 e_0 (τ_{Cd2}).

(the internal solution was 115 mM Na^+ for both traces). For the upper trace, where the external solution also contained 115 mM Na^+, partial recovery is visible after a 500-ms return to holding potential. By contrast, in the lower trace obtained with Tris-Ringer as the external solution, there was no evident recovery from C-type inactivation during this same interpulse interval. Note that in this lower trace, the second depolarization produces an apparently monoexponential approach to the same steady state current level as seen in the first pulse. We conclude that this second depolarizing step induces reactivation of channels that are still C-type inactivated and, since they activate to the same level as the steady state current, it appears that these channels remain C-type inactivated despite this activation process. Thus, in appropriate conditions, channels can both close (Fig. 6) and reopen (Fig. 7) without necessarily recovering from C-type inactivation.

The voltage sensitivity of reactivation in C-type inactivated channels is addressed in Figs. 7, *B* and *C*. In Fig. 7 *B*, the depolarization was varied from −30 to +80 mV to explore the voltage sensitivity of this reactivation process. Fig. 7 *C* shows the activation time constants (τ_{Ca}) obtained from monoexponential fits to currents at test potentials sufficient to generate measurable reactivation under these conditions. From this semilogarithmic plot we note an e-fold change in time constant in 22.3 mV, indicating an effective reactivation valence of ~1 e_0. This value is substantially greater than the ~0.3 e_0 reported for reactivation of noninactivated *Shaker* channels by Zagotta et al. (1994*a*), suggesting that there is some underlying difference between the mechanisms of reactivation in normal and C-type inactivated channels.

Fig. 7 *A* has shown effects of changes in external solutions on rates of recovery from C-type inactivation. We next explore the more complex effects that can arise after changes in internal solutions as a result of combinations of internal K^+ block and changes in the onset and recovery rates of C-type inactivation. Fig. 8 shows six consecutive traces obtained from the same patch, separated at 15-s intervals. In all cases, the external solution was Tris-Ringer. Fig. 8 *A*, *i* and *ii* was obtained using 114 mM Na^+ and 1 mM K^+ in the bath, which was then changed to a K^+-free, 115 mM Na^+ solution for Fig. 8 *B*, *i* and *ii*. Finally, the internal solution was switched back to 114 mM Na^+ and 1 mM K^+ for Fig. 8 *C, i* and *ii*. In Fig. 8 *A, i*, in the presence of 1 mM K^+, a fast C-type inactivating outward K^+ current is visible, followed by a small but detectable steady state current. Recovery from C-type inactivation is fast enough, in the presence of internal K^+ ions, for Fig. 8 *A, ii* to show almost complete recovery of the initial outward K^+ current, although some accumulation of inactivation is noticed despite the 15-s interpulse interval. After washout of internal K^+, Fig. 8 *B, i* shows an initial fast inactivating Na^+ current followed by a substantial steady state current. However, in Fig. 8 *B, ii,* we see that recovery from C-type inactivation has been markedly slowed in the absence of internal K^+, and there is no evidence of any recovery of the fast decaying initial current in this trace. By contrast, Fig. 8 *B, ii* now shows the slow rising phase of activation characteristic of C-type inactivated chan-

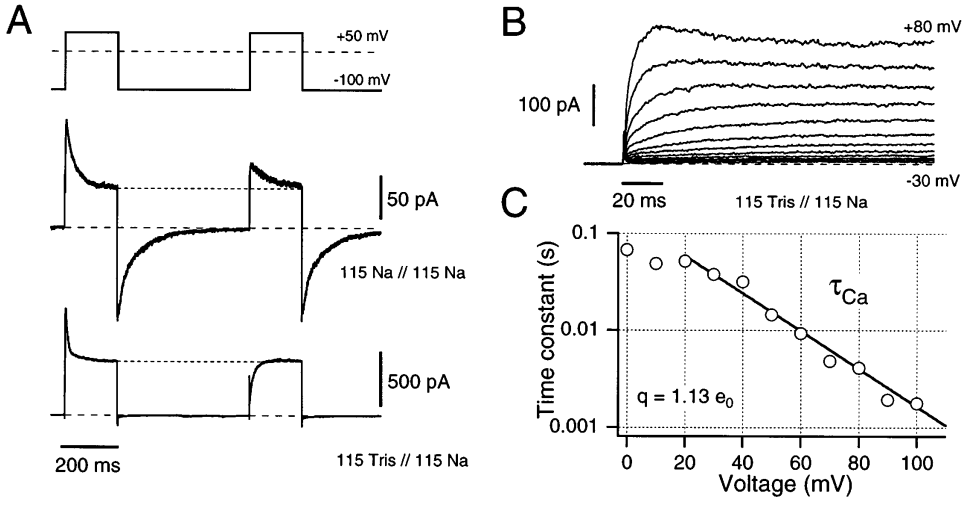

FIGURE 7. Activation of ionic current through C-type inactivated channels. Recovery from C-type inactivation is affected by external cations (*A*). Double-pulse experiments were performed in the indicated solutions. The duration of the interpulse interval at −100 mV was chosen such that the slow tail currents in Na/Na solutions reach the baseline. In Na/Na solutions (*top*) depolarization after complete tail current deactivation shows only partial recovery from inactivation. In Tris/Na solutions (*bottom*), no significant recovery from inactivation is visible. Instead, slow, mono-exponential reactivation to the same steady state level as in the first pulse is observed (*dashed lines*). (*B*) Activation of current through C-type inactivated channels is shown in Tris/Na solutions in response to depolarizations from −100 mV to voltages between −30 and +80 mV in steps of 10 mV. The depolarizations were given in rapid succession such that no marked recovery from inactivation occurred (see *A*). The activation kinetics (under these conditions of steady state inactivation) were estimated by fitting single-exponentials functions to the data. The resulting time constants are plotted in *C* as a function of the test potential. The straight line corresponds to a single exponential function in this semilogarithmic plot. The slope of this line yields an estimate for the apparent gating charge associated with the process of reactivation of 1.13 e_0.

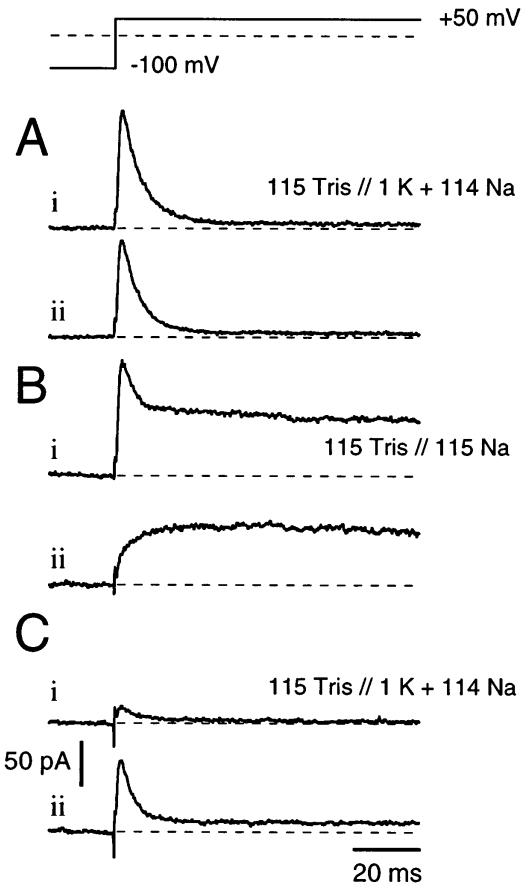

FIGURE 8. Effects of internal K^+ ions on recovery from C-type inactivation. Currents were recorded in the absence of extracellular permeating ions (Tris-Ringer), individual traces being separated by 15-s intervals. Between *A*, *B*, and *C*, bath solutions were altered as indicated. In *A*, in the presence of 1 mM internal K^+, channels undergo rapid and complete inactivation (*A, i* and *ii*). Switching to K^+-free 115 mM internal Na^+ solutions results in a similarly fast inactivation (*B, i*) that falls to a steady state value that indicates continued Na^+ permeation through C-type inactivated channels (see also Fig. 7 *A*). The next pulse in Na^+-solution (*B, ii*) shows no recovery from inactivation, thus this trace shows only activation of C-type inactivated channels (as in Fig. 7 *B*). Switching back to K^+-containing internal solutions reveals almost complete inactivation (*C, i*). However, the final pulse (*C, ii*) shows partial recovery of "normal" inactivation.

nels (see Fig. 7 *B*). During reapplication of 1 mM internal K^+, recovery from C-type inactivation is accelerated but still appears incomplete in Fig. 8 *C, ii,* taken ~30 s after the solution exchange.

Thus, *Shaker* channels appear capable of both opening and closing while remaining C-type inactivated, although with altered kinetics and perhaps through different pathways than those used by normal, noninactivated channels.

DISCUSSION

Previous studies of C-type inactivation in *Shaker* channels have clarified the functional differences between this slow inactivation mechanism and the mechanism of fast, N-type inactivation (Hoshi et al., 1990, 1991). Additionally, this inactivation mechanism has been found to be affected by site-directed mutations in the S6 segment (Hoshi et al., 1991; Holmgren et al., 1997), as well as in the pore domain (López-Barneo et al., 1993; Schlief et al., 1996). Specifically, Schlief et al. (1996) concluded that the externally facing residue at position 448 becomes more accessible during C-type inactivation, while evidence favoring a cooperative action between monomers in the initiation of C-type inactivation has been provided by several groups (Ogielska et al., 1995; Panyi et al., 1995). Finally, a cysteine cross-linking study has demonstrated that C-type inactivation involves conformational changes in the outer mouth of the pore indicating a structural constriction of the outer mouth, potentially sufficient to produce long-term closure of the ion-conducting pathway (Liu et al., 1996). In contrast to the hypothesis that C-type inactivation is accompanied by a "collapse" of the pore leading to a virtually closed channel, we show here that channels remain capable of conducting impermeant Na^+ and Li^+ ions in the C-type inactivated state, provided that internal blocking effects of K^+ are first removed by careful washout of K^+ from the internal medium.

The critical evidence required to reach this conclusion has involved demonstrating, first, that the rapid inactivation found using K^+-free, Na^+-substituted internal and external solutions has the characteristic properties of the C-type inactivation found in normal physiological solutions and, second, that the Na^+ permeation found under these conditions is occurring through inactivated channels rather than through a population of normal channels in equilibrium with the inactivated population. A residual population of noninactivated channels must be present at negative test potentials, although C-type inactivation appears to become almost complete at potentials $>+20$ mV. However, previous work has shown that the same impermeant ions will also pass through normal, noninactivated K^+ channels provided that K^+ is first removed from the internal solution (Callahan and Korn, 1994; Ikeda and Korn, 1995; Ogielska and Aldrich, 1997). Since both noninactivated and C-type inactivated channels appear to be Na^+ permeable in the absence of internal K^+, we show here (see Fig. 2) that C-type inactivation can be detected from marked and characteristic changes in tail current waveform that far exceed the rate changes previously reported to result from substitutions in permeating ion species (Zagotta et al., 1994*a*). Thus, Fig. 2 shows fast initial Na^+ tail currents through noninactivated channels converting to slowly deactivating Na^+ tail currents through C-type inactivated channels.

Nevertheless, the rapid non–N-type inactivation occurring in K^+-free solutions could be associated with

some alternative inactivated state, rather than with the classic, slow onset C-type states that have been characterized in physiological internal and external solutions. Therefore, we demonstrate that equivalent tail current waveform changes occur during entry into C-type states in more physiological solutions (Fig. 3) and that these changes in tail current kinetics are correlated with coincident changes in P_K, such that C-type inactivated channels become effectively impermeant to K^+ ions (in all solutions). However, in K^+-free internal solutions, channels remain permeable to Na^+ and Li^+ as they enter into C-type inactivated states (Fig. 4), indicating that the lack of permeation by these ions in physiological solutions arises from internal K^+ block (Fig. 5). We note that large inward Na^+ tail currents remain unblocked by 2.5 mM external K^+ (see Fig. 3, *C* and *D*) and suspect that access to this blocking site may prove to be substantially asymmetrical, although further and more quantitative studies will be required to confirm this point.

The Na^+ tail currents that follow inactivating prepulses indicate that channels must close within ~500 ms even at −100 mV, although complete recovery from C-type inactivation takes ~15 s even at these negative return potentials. It seems clear, therefore, that these tail currents represent the closing (deactivation) of channels that remain predominantly in a C-type inactivated state (see Fig. 6). Similarly, we have demonstrated reactivation of C-type inactivated channels from a closed to a Na^+-conducting C-type state (see Fig. 7) on subsequent depolarization. These deactivation and reactivation rates are considerably slower than the corresponding rates for normal, noninactivated channels. However, the voltage sensitivity of deactivation seems similar to the apparent gating valence of ~1 e_0 reported for *Shaker* channels by Zagotta et al. (1994*a*). Thus, the deactivation process characterized by the falling phase of these Na^+ tail currents may be similar to that which occurs in noninactivated channels. By contrast (see Fig. 7 *C*), reactivation seems to be substantially more voltage sensitive in these C-type inactivated channels (~1 e_0) than in noninactivated *Shaker* channels (Zagotta et al., 1994*a*, 1994*b*) over the potential range of +20 to +100 mV. It seems possible that reactivation of C-type inactivated channels involves additional transitions that are not resolved as separate kinetic components in the ionic current records. Finally, we demonstrate (see Fig. 8) some of the complex effects of internal solution changes on conduction through C-type inactivated channels.

In the nonstandard solutions used here, deactivation and reactivation of channels that have entered C-type states generates the expected changes in macroscopic currents, albeit with modified kinetics. By contrast, in physiological solutions C-type deactivation and reactivation will be characterized only by gating currents. Similarly, single-channel records obtained in physiological solutions would be expected to show only entry into or escape from long "closed" states, although such closing would be a consequence of changed permeation properties rather than of true channel closure. Unfortunately, the very low permeation for Na^+ and Li^+ during C-type inactivation will make it difficult to provide a direct test of this conclusion from single-channel records.

It seems mechanistically significant that C-type inactivation develops with time constants that vary from seconds (in symmetric 115-mM K^+ solutions) to tens of milliseconds (in symmetric 115-mM Na^+ solutions). In view of this wide range of rates, we speculate that C-type inactivation is an intrinsically fast process (with a time constant in the range of microseconds) that is modulated by binding of K^+ ions (and to a lesser extent by Na^+ ions). For example, activation of the charge-carrying S4 segments could initiate both channel opening and a cooperative process, which, if unopposed, will trigger conformational changes in the region of the external "filter," thus reducing the permeability of the channel to K^+ ions. Presuming this conformational change is prevented by the presence of a K^+ ion at this external site, the rate of C-type inactivation would be determined by the availability of K^+ ions in this region, becoming faster as K^+ concentration is reduced. Since this site lies in the permeation path, it should be accessible from both external and internal sides of the membrane, in open, conducting channels, and internal K^+ might be expected to substitute for external K^+, as shown in Fig. 1. Furthermore, this hypothesis predicts that C-type inactivation will be fast in symmetric Na^+ solutions, faster in Tris/Na solutions (see Fig. 7), and presumably even faster (or not measurable) in Tris/Tris solutions.

The reduced efficacy of other ion species in slowing C-type inactivation could be due either to the reduced dwell time of these ions or to their reduced ability to slow the external conformational change. The occupancy hypothesis (Matteson and Swenson, 1986; Sala and Matteson, 1991; Zagotta et al., 1994*a*) suggests that changes in dwell time within the channel are important determinants of the deactivation rate. We note that K^+ has the shortest dwell time (according to this hypothesis) but has the highest efficacy in preventing/delaying C-type inactivation. Since the order of efficacy is opposite to that which would be predicted on the basis of the occupancy hypothesis, we conclude that efficacy is determined through ion specificity (i.e., by closeness of interaction with critical residues in the outer selectivity filter) rather than by a nonspecific dwell time effect on channel gating.

In conclusion, we restate the hypothesis that seems to provide the most elegant explanation of the results obtained in the present study. Permeation, in *Shaker* channels, is primarily determined by the properties of the

externally located "selectivity filter," which is normally highly selective for K^+ over Na^+ ions. However, during C-type inactivation, this external filter changes its properties; i.e., greatly reducing K^+ permeability while leaving Na^+ permeability relatively unchanged. We presume that this change in relative permeabilities is the primary mechanism of the "inactivation" seen in C-type inactivated states. Nevertheless, Na^+ permeation does not occur in C-type inactivated states in physiological solutions, due to blocking actions of internal K^+ ions. Removal of K^+ from the internal solution thus permits limited permeation of the channel by ions such as Na^+ and Li^+ and, in a more general sense, permits direct evaluation of the selectivity of the external filter.

We thank K. McCormack for providing us with *Sh*Δ. The valuable technical assistance of A. Grimm, A. Rossner, A. Hakeem, and M. Henteleff is appreciated.

S.H. Heinemann was partially supported by a Human Frontier Science Program grant. J.G. Starkus was supported in part by National Institutes of Health grant RO1-NS21151, by a grant from the American Heart Association (Hawaii Affiliate), by Pacific Biomedical Research Center Bridging Funds, and by the Max Planck Society. M.D. Rayner was supported by grants from the American Heart Association (Hawaii Affiliate) and from the Queen Emma Foundation.

Original version received 11 July 1997 and accepted version received 5 September 1997.

REFERENCES

Armstrong, C.M., F. Bezanilla, and E. Rojas. 1973. Destruction of sodium conductance inactivation in squid axons perfused with pronase. *J. Gen. Physiol.* 62:375–391.

Armstrong, C.M., and F. Bezanilla. 1977. Inactivation of the sodium channel. II. Gating current experiments. *J. Gen. Physiol.* 70:567–590.

Callahan, M.J., and S.J. Korn. 1994. Permeation of Na^+ through a delayed rectifier K^+ channel in chick dorsal root ganglion neurons. *J. Gen. Physiol.* 104:747–771.

Hamill, O.P., A. Marty, E. Neher, B. Sakmann, and F.J. Sigworth. 1981. Improved patch-clamp techniques for high-resolution current recording from cells and cell-free membrane patches. *Pflügers Arch.* 391:85–100.

Heinemann, S.H., F. Conti, and W. Stühmer. 1992. Recording of gating currents from *Xenopus* oocytes and gating noise analysis. *In* Ion Channels. B. Rudy and L.E. Iverson, editors. Academic Press, Inc., Orlando, FL. 207:353–368.

Holmgren, M., P.L. Smith, and G. Yellen. 1997. Trapping of organic blockers by closing of voltage-dependent K^+ channels. *J. Gen. Physiol.* 109:527–535.

Hoshi, T., W.N. Zagotta, and R.W. Aldrich. 1990. Biophysical and molecular mechanisms of *Shaker* potassium channel inactivation. *Science (Wash. DC).* 250:533–538.

Hoshi, T., W.N. Zagotta, and R.W. Aldrich. 1991. Two types of inactivation in *Shaker* K^+ channels: effects of alterations in the carboxy-terminal region. *Neuron.* 7:547–556.

Ikeda, S., and S.J. Korn. 1995. Influence of permeating ions on potassium channel block by external tetraethylammonium ions. *J. Physiol. (Lond.).* 486:267–272.

Iverson, L.E., and B. Rudy. 1990. The role of divergent amino and carboxyl domains on the inactivation properties of potassium channels derived from the *Shaker* gene of *Drosophila*. *J. Neurosci.* 10:2903–2916.

Liu, Y., M.E. Jurman, and G. Yellen. 1996. Dynamic rearrangement of the outer mouth of a K^+ channel during gating. *Neuron.* 16:859–867.

Levy, D.L., and C. Deutsch. 1996. Recovery from C-type inactivation is modulated by extracellular potassium. *Biophys. J.* 70:798–805.

López-Barneo, J., T. Hoshi, S.H. Heinemann, and R.W. Aldrich. 1993. Effects of external cations and mutations in the pore region on C-type inactivation of *Shaker* potassium channels. *Receptors Channels.* 1:61–71.

Matteson, D.R., and R.P. Swenson. 1986. External monovalent cations that impede the closing of K channels. *J. Gen. Physiol.* 87:795–816.

McCormack, K., W.J. Joiner, and S.H. Heinemann. 1994. A characterization of the activating structural rearrangements in voltage-dependent *Shaker* K^+ channels. *Neuron.* 12:301–315.

Meyer, R., and S.H. Heinemann. 1997. Temperature and pressure dependence of *Shaker* K^+ channel N- and C-type inactivation. *Eur. Biophys. J.* In press.

Ogielska, E.M., W.N. Zagotta, Z. Hoshi, S.H. Heinemann, J. Haab, and R.W. Aldrich. 1995. Cooperative subunit interactions on C-type inactivation of K channels. *Biophys. J.* 69:2449–2457.

Ogielska, E.M., and R.W. Aldrich. 1997. A single amino acid substitution in the S6 of *Shaker* decreases potassium affinity and allows for sodium permeation in the absence of potassium. *Biophys. J.* 72:*A*233. (Abstr.)

Panyi, G., Z. Sheng, and C. Deutsch. 1995. C-type inactivation of a voltage-gated K^+ channel occurs by a cooperative mechanism. *Biophys. J.* 69:896–903.

Rudy, B. 1978. Slow inactivation of the sodium conductance in squid giant axons. Pronase resistance. *J. Physiol. (Lond.).* 283:1–21.

Sala, S., and D.R. Matteson. 1991. Voltage-dependent slowing of K channel closing kinetics by Rb^+. *J. Gen. Physiol.* 98:535–554.

Schlief, T., R. Schönherr, and S.H. Heinemann. 1996. Modification of C-type inactivation *Shaker* potassium channels by chloramine-T. *Pflügers Arch.* 431:483–493.

Steffan, R., C. Hennesthal, and S.H. Heinemann. 1997. Voltage-gated ion channels: analysis of nonideal macroscopic current data. *In* Ion Channels. P.M. Conn, editor. Academic Press, Inc. Orlando, FL. In press.

Zagotta, W.N., T. Hoshi, and R.W. Aldrich. 1990. Restoration of inactivation in mutants of *Shaker* potassium channels by a peptide derived from ShB. *Science (Wash. DC).* 250:568–571.

Zagotta, W.N., T. Hoshi, J. Dittman, and R.W. Aldrich. 1994*a*. *Shaker* potassium channel gating. II. Transition in the activation pathway. *J. Gen. Physiol.* 103:279–319.

Zagotta, W.N., T. Hoshi, and R.W. Aldrich. 1994*b*. *Shaker* potassium channel gating. III. Evaluation of kinetic models for activation. *J. Gen. Physiol.* 103:321–362.